

First-principles study of the minimal model of magnetic interactions in Fe-based superconductors

J. K. Glasbrenner

National Research Council/Code 6393, Naval Research Laboratory, Washington, D.C. 20375, USA

J. P. Velev

*Department of Physics, Institute for Functional Nanomaterials, University of Puerto Rico, San Juan, Puerto Rico 00931, USA
and Code 6393, Naval Research Laboratory, Washington, D.C. 20375, USA*

I. I. Mazin

Code 6393, Naval Research Laboratory, Washington, D.C. 20375, USA

(Received 8 January 2014; revised manuscript received 28 January 2014; published 21 February 2014)

Using noncollinear first-principles calculations, we perform a systematic study of the magnetic order in several families of ferropnictides. We find a fairly universal energy dependence on the magnetization order in all cases. Our results confirm that a simple Heisenberg model fails to account for the energy dependence of the magnetization in a couple of ways: first, a biquadratic term is present in all cases and, second, the magnetic moment softens depending on the orientation. We also find that hole doping substantially reduces the biquadratic contribution, although the antiferromagnetic stripe state remains stable within the whole range of doping concentrations, and thus the reported lack of the orthorhombicity in Na-doped BaFe_2As_2 is probably due to factors other than a sign reversal of the biquadratic term. Finally, we discover that even with the biquadratic term, there is a limit to the accuracy of mapping the density functional theory energetics onto Heisenberg-type models, independent of the range of the model.

DOI: [10.1103/PhysRevB.89.064509](https://doi.org/10.1103/PhysRevB.89.064509)

PACS number(s): 74.70.Xa, 74.25.Ha, 74.20.Mn

I. INTRODUCTION

Fe-based superconductors are only the second family, after cuprates, of known high- T_c superconductors (HTSCs). The parent compounds of these materials exhibit magnetic ordering at low temperatures and, in their phase diagrams, the magnetic phase is proximate to the superconducting phase. The two orders are intimately related as the superconductivity emerges when magnetism is suppressed, for instance, by doping. Therefore, it is generally believed that magnetic fluctuations in these systems are the likely driver of the pairing mechanism [1,2]. Magnetic order is also accompanied (with a notable exception discussed later) by a structural phase transition, and there are compelling arguments that this is also driven by magnetism: (1) density functional calculations quantitatively reproduce the observed orthorhombic distortions, including the amplitude and the counterintuitive sign, and also reproduce a qualitatively different distortion in FeTe [3], and (2) the same calculations fail to produce any distortion in the absence of magnetism. The seemingly counterintuitive fact that the structural instability sometimes occurs at a temperature slightly above the magnetic transition is, in fact, consistent with this concept because long-range magnetic order is sufficient, but not necessary, for breaking the global C_4 symmetry: it is enough to unequally populate magnetic fluctuations with different \mathbf{k} vectors. These can be described as fluctuating domain walls in an itinerant picture [4] or as “order from disorder” in the local-moment picture (see Refs. [5–7]; for a review, see Ref. [8]). This picture is also consistent with observations of fluctuations breaking charge [9] and spin [10] C_4 symmetry locally, well above the Néel temperature.

The local-moment picture has the advantage of being analytically solvable and simple; Heisenberg-like models are a popular way to approach the magnetism of Fe-based HTSCs.

This can be considered a reasonable approach since, with a sufficient number of parameters, any sort of magnetic interaction can be mapped onto a local-moment model. The simplest possible model is a Heisenberg-type interaction between the first and second nearest neighbors [5–7]. This model has the desired property that symmetry breaking *always* occurs above the Néel temperature, although this splitting diminishes as the magnetic interaction becomes more three dimensional. While the model replicates some physical properties of Fe-based HTSCs, there is a serious problem that is often overlooked. The essential physics of this approach can be described as follows [8]: an Fe plane can be viewed as a bipartite lattice where the only interaction within each sublattice is the second-nearest-neighbor exchange J_2 , while the only interaction between the sublattices is J_1 . As illustrated in Fig. 1, exchange interaction constant J_2 , if $J_2 > J_1/2$, generates a checkerboard antiferromagnetic (AFM) pattern in each sublattice, while the interaction between the sublattices cancels completely, which holds not only for an arbitrary J_1 but also for any Heisenberg interaction of an arbitrary range. In Ref. [5], it was shown that after integrating out quantum fluctuations, a nearest-neighbor biquadratic term of the form $K(\mathbf{S}_i \cdot \mathbf{S}_j)$ appears in the effective Hamiltonian, with $K > 0$ and of the order of $10^{-4}J$. This lifts the infinite degeneracy of the ground state, leaving a double-degenerate state of ferromagnetic stripes running along one of the two crystallographic directions with AFM alternation, matching the ground state of the ferropnictides of interest. However, the small amplitude of K is unphysical, making this result purely academic and not applicable to any real material.

There is another profound problem with the Heisenberg model. Even though it formally generates the correct ground states for ferropnictides, it fails to explain the double stripe structure of FeTe; to do so requires introducing the third-

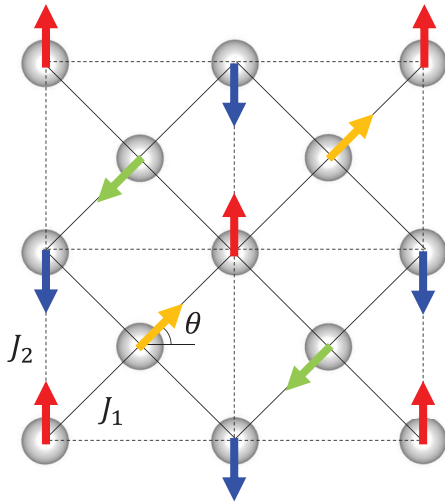


FIG. 1. (Color online) Schematic view of the two-dimensional Fe planes in the Fe-based superconductors. The first- (J_1) and second- (J_2) nearest-neighbor exchange interactions are shown in solid and dashed lines. The moments on the two sublattices form an antiferromagnetic checkerboard pattern and, in our calculations, the moments on one sublattice are rotated by an angle θ relative to the other. The antiferromagnetic stripe patterns correspond to $\theta = 0^\circ$ and $\theta = 180^\circ$.

nearest-neighbor exchange J_3 , which is found to be of the same order as J_1 and J_2 , which is a result inconsistent with the superexchange picture. Even worse, in order to fit both the ground-state and the spin-wave spectra, one needs to split the nearest-neighbor exchange into two inequivalent parameters, J_{1a} and J_{1b} . The two parameters end up being different from each other, sometimes even changing sign [11]. This implies that not only do the exchange constants change qualitatively from compound to compound, but that they have a strong, counterintuitive dependence on temperature; the inequivalent parameters J_{1a} and J_{1b} , above the Néel temperature, become equivalent as required by symmetry, i.e., $J_{1a} = J_{1b}$. This bizarre and inconsistent behavior is the death knell for using the superexchange theory to model the Fe-based HTSCs, as there is no plausible physical mechanism that can explain the dramatic temperature dependence of the superexchange constants.

Density functional theory (DFT) calculations, when mapped onto the same Heisenberg model, yield similar exchange constants, including the splitting of the nearest-neighbor exchange [12,13]. This indicates that DFT is correct in its description of the Fe-based HTSCs (it can quantitatively explain the spin-wave spectrum, for example), suggesting that this methodology can be used to resolve the exchange constants conundrum. In fact, the necessary calculations have been reported at a very early stage, yet were largely overlooked [14]. Instead of an unphysical model with only superexchange terms, the same DFT calculations can be mapped with good accuracy onto an isotropic ($J_{1a} = J_{1b}$) Heisenberg model which includes a biquadratic term (formally the same as found in Ref. [5]) with an amplitude of $K \sim J_1, J_2$. Moreover, noncollinear DFT calculations with one magnetic sublattice rotated with respect to the other (see Fig. 1) can only be mapped onto this model. It was then shown that this biquadratic,

isotropic Hamiltonian with temperature-independent parameters is an excellent model of the magnetic properties of Fe-based HTSCs at any temperature, including the spin-wave spectra [15]. The model also is consistent with an orthorhombic transition occurring above the magnetic one.

These discoveries yielded a much more robust description of the magnetic behavior of the Fe-based HTSCs, which includes a consistent explanation of the orthorhombic distortion. Instead of a minuscule “order-from-disorder” term appearing to drive the physics of these systems, we have a sizable biquadratic term on the mean-field level. So what is missing at this point? To date, there is no body of information about the biquadratic term. Important questions include the following: How variable is it from compound to compound? How does it depend on doping? Can it change sign, leading to a noncollinear ground state while preserving tetragonal symmetry? At the present moment, only some answers are available. In Ref. [14], only two compounds were studied and the uncontrollable atomic spheres approximation was used. While there is no question that the obtained results were qualitatively correct, their quantitative accuracy remained unclear. Beyond that, in Ref. [16], it was demonstrated that the biquadratic term depends on the details of a material’s band structure. Using accurate full-potential DFT calculations with linear muffin-tin orbitals, it was shown that the biquadratic term is negative in stoichiometric KFe_2Se_2 , which is a hypothetical material. The term is also dependent on the size of the local Fe moment (or, equivalently, the Fe-As/Se bond-length distance), again indicating the necessity for accurate calculations. Finally, the ultimate question that can be posed is whether the total energy is mappable onto the pair interaction at all, linear or quadratic, in $\mathbf{S}_i \cdot \mathbf{S}_j$. This is always taken for granted, but there is no *a priori* reason for that to be true in an itinerant system.

In DFT, the change in energy between different magnetic patterns accumulates via integration over the entire occupied portion of the Fe band, which extends several eV below the Fermi energy. Profound orbital reordering induced by magnetism leads to the observed stripe order being lower in energy compared to other patterns [17,18] and, by extension, affects the exchange constants obtained by mapping. These complex changes in the electronic structure are responsible for the anisotropy in the J -only model and for the large biquadratic term in the J - K model, and also for the longer-range interactions in FeTe. This contrasts with the simplistic superexchange model where both K and J_3 appear only as higher-order terms and must be much smaller than J_1 and J_2 .

Resolving the incomplete understanding of the biquadratic term has become even more important after an intriguing experimental report that the orthorhombic distortion disappears in a small part of the $\text{Ba}_{1-x}\text{Na}_x\text{Fe}_2\text{As}_2$ phase diagram, while magnetic order remains [19]. The authors favor the plausible explanation that the biquadratic term changes sign in that region, generating the noncollinear structure shown in Fig. 1(c) of Ref. [19]. An alternative explanation would be that the magnetoelastic coupling that drives the orthorhombic distortion becomes small and the (still existing) C_2 symmetry breaking goes undetected.

The former explanation, that the biquadratic term changes sign upon doping, was supported by the calculations of

TABLE I. Summary of the crystallographic symmetry groups, lattice structure (lattice constants a and c and fractional coordinates z of the nonmagnetic planes), Fe-Fe/Fe-As(Se) bond lengths, the fitted parameters of Eqs. (2) and (3), and the energy change due to the softening of the magnetic moment for all of the studied compounds.

Compound	Sym. Group	a (Å)	c (Å)	$z_{\text{As,Se}}$ ($z_{\text{Li,Na,La}}$) (frac.)	$d_{\text{Fe-Fe}}$ (Å)	$d_{\text{Fe-As(Se)}}$ (Å)	$M(0)$ (μ_B)	K (meV)	J_{\perp} (meV)	$E(0) _{M(90)} - E(0) _{M(0)}$ (meV)
FeSe	$P4/nmm$	3.803	6.084	0.2708	2.689	2.516	2.72	9.67		-0.04
LiFeAs	$P4/nmm$	3.793	6.366	0.2365 (0.6541)	2.682	2.421	1.85	9.75		4.21
NaFeAs	$P4/nmm$	3.949	7.040	0.2028 (0.6460)	2.793	2.437	2.18	15.43		7.30
LaFeAsO	$P4/nmm$	4.037	8.742	0.1513 (0.6415)	2.854	2.413	2.09	13.24		4.97
SrFe ₂ As ₂	$I4/mmm$	3.930	12.324	0.3604	2.779	2.390	1.94	10.57	0.79	2.78
CaFe ₂ As ₂	$I4/mmm$	3.896	11.683	0.3665	2.755	2.376	1.83	9.39	1.33	1.58
KFe ₂ As ₂	$I4/mmm$	3.842	13.860	0.3525	2.716	2.389	2.46	6.36	0.40	9.48
KFe ₂ Se ₂	$I4/mmm$	3.914	14.037	0.3434	2.767	2.355	2.47	-3.29	-0.05	0.48
BaFe ₂ As ₂	$I4/mmm$	3.942	13.021	0.3545	2.791	2.397	1.99	10.84	0.23	3.33
Ba _{0.9} Na _{0.1} Fe ₂ As ₂	"	"	"	"	"	"	1.96	9.85	0.21	4.04
Ba _{0.8} Na _{0.2} Fe ₂ As ₂	"	"	"	"	"	"	1.94	8.73	0.22	4.73
Ba _{0.7} Na _{0.3} Fe ₂ As ₂	"	"	"	"	"	"	1.93	7.80	0.26	5.30
Ba _{0.6} Na _{0.4} Fe ₂ As ₂	"	"	"	"	"	"	1.93	7.16	0.30	7.04
Ba _{0.5} Na _{0.5} Fe ₂ As ₂	"	"	"	"	"	"	1.94	5.56	0.24	5.37
Ba _{0.4} Na _{0.6} Fe ₂ As ₂	"	"	"	"	"	"	1.96	4.42	0.21	6.15
Ba(Fe _{0.5} Co _{0.5}) ₂ As ₂	"	"	"	"	"	"	1.27	0.94	0.04	

Chubukov and Eremin [20], who derived a biquadratic term in the linear response regime. The problem with this approach is that it contradicts the DFT finding [3,17,18] that the energy associated with magnetic interaction accumulates over a large energy window, and that the local moments of Fe remain large throughout the entire phase diagram. On the other hand, knowing that magnetic ordering has a strong effect on the density of states and the orbital composition of the Fe bands, it is plausible that the sign of the biquadratic interaction parameter is not fixed and could change upon doping. As previously discussed, the results of Ref. [16] show that for the hypothetical KFe₂Se₂ compound, which can be viewed as a case of extreme hole doping, the biquadratic term does indeed change sign.

Our goal in this paper is to make a systematic investigation of the biquadratic interaction in representative Fe-pnictide and Fe-chalcogenide families to address the variability of the biquadratic interaction. For this investigation, we use the all-electron, full-potential linear augmented plane waves (FLAPW) method. We find that the biquadratic parameter can vary within large limits, but that it does not change sign in the accessible ranges of doping. We conclude, in particular, that the observed lack of an orthorhombic distortion in the Na-doped BaFe₂As₂ compound in Ref. [19] is likely due to the inaccessibility of the tetragonal symmetry breaking by the experimental tools used in that work.

II. METHODS

We investigate the magnetic order in representative compounds from different families of the iron-based superconductors: FeSe for the 11 family; LiFeAs and NaFeAs for the 111 family; BaFe₂As₂, BaFeCoAs₂, CaFe₂As₂, SrFe₂As₂, KFe₂As₂, and KFe₂Se₂ for the 122 family; and LaFeAsO for the 1111 family. The magnetic order is modeled using the J_1 - J_2 - K model

Hamiltonian,

$$H = J_1 \sum_{nn} \mathbf{S}_i \cdot \mathbf{S}_j + J_2 \sum_{nnn} \mathbf{S}_i \cdot \mathbf{S}_j - K \sum_{nn} (\mathbf{S}_i \cdot \mathbf{S}_j)^2. \quad (1)$$

We use the experimentally determined crystal structures when available [21]; for the hypothetical material KFe₂Se₂, we used the lattice constants from Ref. [16]. A summary of the symmetry groups, lattice constants, and Fe-Fe and Fe-As(Se) bond lengths for all of the materials is found in Table I. The FeAs(Se) planes are stacked along the c axis separated by a nonmagnetic filler plane, except for the 11 compound FeSe, which consists only of FeSe planes. The Fe layers form a two-dimensional square lattice and the ground-state magnetic order has been confirmed both experimentally [22] and theoretically [14] to be AFM stripe order, as schematically represented in Fig. 1 (stripe order corresponds to $\theta = 0$ or $\theta = 180^\circ$). In all cases, in order to accommodate the AFM stripe pattern, we double the cell in the xy plane ($\sqrt{2} \times \sqrt{2}$).

In order to study the biquadratic coupling, we allow the angle θ between the two Fe sublattices to vary. The angle θ , as depicted in Fig. 1, gradually interpolates between two equivalent stripe states with $\mathbf{q} = (1,0)$ and $\mathbf{q} = (0,1)$. According to the biquadratic model in Eq. (1), the angular energy dependence $\Delta E(\theta) = E(\theta) - E(0)$ of the 11, 111, and 1111 families is predicted to be

$$\Delta E(\theta) = 4K \sin^2 \theta. \quad (2)$$

The 122 family belongs to a centered symmetry group, and therefore rotating θ by 180° takes the system from one stripe pattern to another, inequivalent one. The two differ by the stacking order along c and the energy difference is proportional to the interplanar exchange constant J_{\perp} . Taking this into account, the angular energy dependence for the 122 family is

$$\Delta E(\theta)_{122} = 4K \sin^2 \theta - 16J_{\perp} \sin^2 \left(\frac{\theta}{2} \right). \quad (3)$$

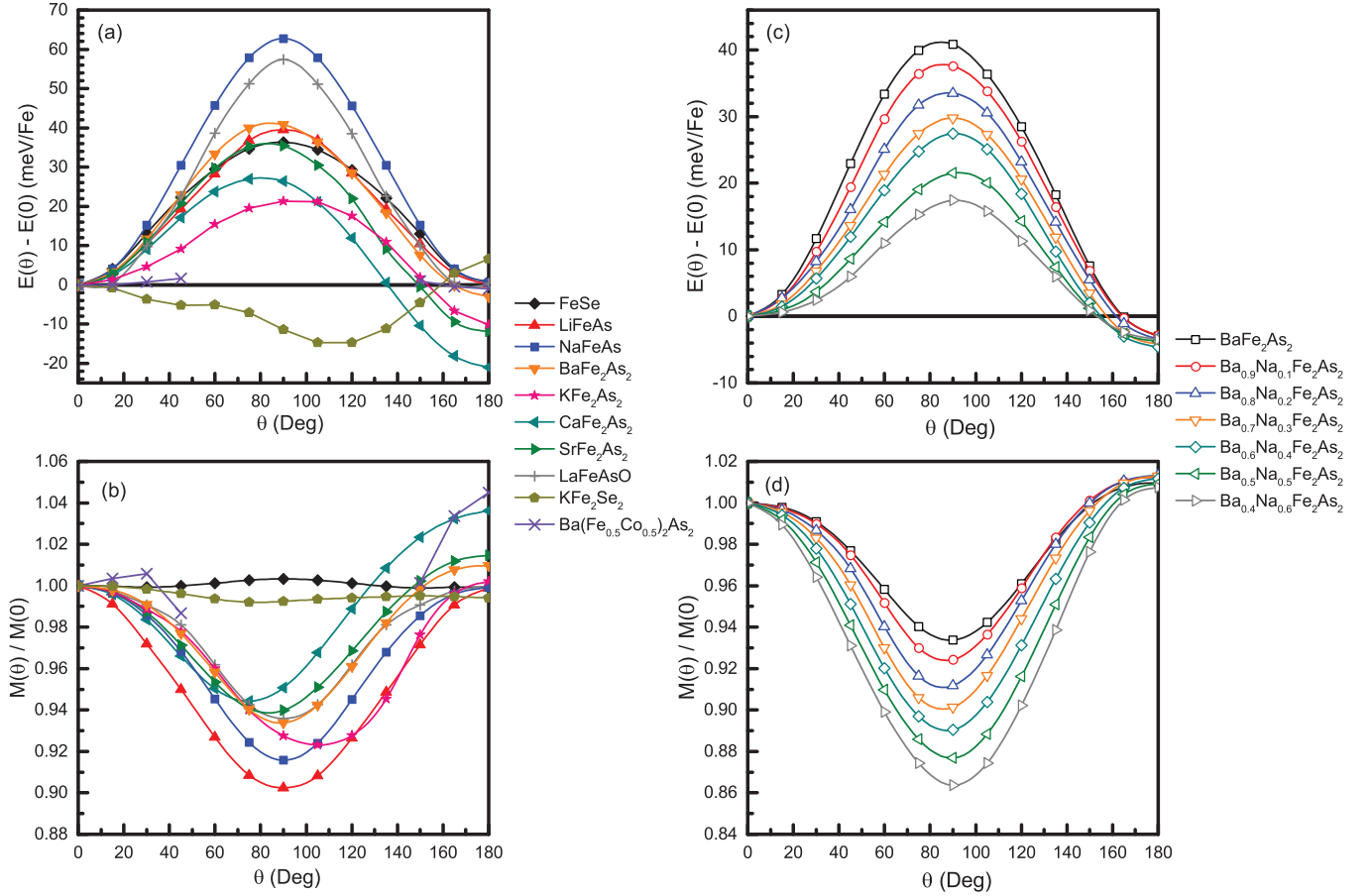


FIG. 2. (Color online) The energy $E(\theta) - E(0)$ and the normalized moment $M(\theta)/M(0)$ as a function of the relative angle θ of the two magnetic subsystems. Note that in all instances, the lines are a guide to the eye and do not represent a fit. (a) The angular dependence of the energy for compounds belonging to the 11, 111, 122, and 1111 families of superconductors. (b) The angular dependence of the normalized moments belonging to the 11, 111, 122, and 1111 families of superconductors. (c) The angular dependence of the energy for different doping levels of the 122 compound BaFe_2As_2 . (d) The angular dependence of the normalized moments for different doping levels of the 122 compound BaFe_2As_2 .

This splits the degeneracy of the $\theta = 0$ and $\theta = 180^\circ$ states by $16J_\perp$.

In order to calculate the angular energy dependence, we perform fully noncollinear first-principles calculations using the ELK code [23]. ELK implements density functional theory (DFT) within a FLAPW basis set with local orbitals. In our calculations, we use the Perdew-Burke-Ernzerhof (PBE) exchange-correlation functional [24]. ELK allows constrained magnetic-moment calculations where the moment direction and/or magnitude can be fixed. To study the effect of hole doping on BaFe_2As_2 , we use the virtual crystal approximation (VCA) in the standard way, in which homogeneous doping is achieved by replacing the Ba atoms with fictitious atoms of fractional nuclear charge between those of Ba and Cs. The density of states (DOS) around the Fermi energy of BaFe_2As_2 is dominated by Fe and As states, and so using VCA has the primary effect of shifting the Fermi energy and removing a fractional number of electrons from the valence band.

Convergence was checked as a function of the size of the k -point mesh. Different size Monkhorst-Pack k -point grids were used for the different families of compounds: $9 \times 9 \times 8$ for 11; $9 \times 9 \times 8$ for 111; $8 \times 8 \times 9$ for 122; and $6 \times 6 \times 4$ for

1111, respectively. Due to the small energy differences, the energy convergence criterion was set to 10^{-7} Ha.

III. RESULTS AND DISCUSSION

We checked the relative energies of the different magnetic orders. In all cases, we obtained that in the FM configuration, the magnetic moment collapses and this configuration is much higher in energy than the AFM configurations. The energy of the checkerboard AFM configuration was found to be higher in energy than the AFM stripe ground state; hole doping decreased the relative energy difference, although the AFM stripe state remained as the ground-state configuration.

The angular dependence of the energy difference $\Delta E(\theta) = E(\theta) - E(0)$ for different compounds is plotted in Fig. 2(a). It is clear that biquadratic coupling is present in all of these compounds. We fitted these results to Eq. (2) for the 11, 111, and 1111 families and Eq. (3) for the 122 family. The fitted parameters are summarized in Table I.

The angular energy dependence of the materials, with the exceptions of KFe_2Se_2 and $\text{Ba}(\text{Fe}_{0.5}\text{Co}_{0.5})_2\text{As}_2$, follow a similar pattern, with the energy difference between the ground stripe state and the least favorable $\theta = 90^\circ$ configuration

varying between 30–60 meV/Fe. Our results for LaFeAsO, BaFe₂As₂, and KFe₂Se₂ agree well with previous calculations [14,16]. The biquadratic interaction constant K is fairly large and positive in most materials (again excepting KFe₂Se₂ and Ba(Fe_{0.5}Co_{0.5})₂As₂) and of the same order as J_1 and J_2 [13,14]. One of the factors that influences K is the Fe-Fe bond length, as K tends to be larger in compounds which have a greater Fe-Fe distance such as LaFeAsO, NaFeAs, and BaFe₂As₂. The interlayer coupling J_{\perp} in the 122 family is about an order of magnitude smaller than K , and the constant varies from material to material.

Ba(Fe_{0.5}Co_{0.5})₂As₂ and KFe₂Se₂ are exceptions to the above trends. Ba(Fe_{0.5}Co_{0.5})₂As₂ was calculated using the VCA and represents electron doping of BaFe₂As₂. This doping softens the ground-state moment by 36% and destabilizes the local moment for angles $45^\circ < \theta < 150^\circ$, in which range it collapses. This level of electron doping also suppresses the biquadratic and interplanar interactions, reducing both by an order of magnitude. KFe₂Se₂, on the other hand, exhibits a negative biquadratic interaction term, in agreement with the Ref. [16] results [25]. While it exhibits a negative K , bulk KFe₂Se₂ is a hypothetical material that cannot be stabilized in experiment [26], so here it just serves as a proof of concept that a negative K is possible.

The softening of the moments shown in Fig. 2(b) contributes to $\Delta E(\theta)$ in a nontrivial way. Modeling the variation of the magnetic moments necessitates the inclusion of J_2 exchange terms in Eqs. (2) and (3), as well as on-site Hund's exchange terms such as $IM(\theta)^2$ (I is the Hund's exchange constant). A simpler way to estimate the importance of the moment softening is to calculate $E(0)|_{M(90)} - E(0)|_{M(0)}$ in the collinear AFM stripe state configuration, i.e., the energy change from reducing the ground-state moment to the self-consistent amplitude at $\theta = 90^\circ$, where the softening is greatest. The final column in Table I reports these calculations. For pnictides, the difference is positive and only a few meV in magnitude. For chalcogenides, the moment softening is slight and accordingly the energy contribution from the softening is also small. For FeSe, the moment amplitude grows slightly at $\theta = 90^\circ$, and there is a corresponding small gain in energy. In all cases, we see that most of the energy change in Fig. 2(a) is driven by the biquadratic term, with only a modest contribution coming from the moment softening.

The angular energy dependence for various levels of hole doping in Ba_{1-x}Na_xFe₂As₂ via the VCA is depicted in Fig. 2(c). A discussion of the validity of using the VCA to address the effect of hole doping on the biquadratic term is included in the Appendix. As is clear in the figure, the biquadratic interaction constant K strongly depends on the degree of hole doping in the material. Going from an undoped system to $x = 0.6$ results in a 60% decrease in K . Extrapolating the hole doping of BaFe₂As₂ to the extreme $x = 1$ case, the biquadratic constant K , however, does not invert and instead nearly vanishes. Because of the similarity of results in other materials, we expect that doping via the VCA would yield similar results in other materials. Of course, in the case of extreme hole doping, it is necessary to allow the lattice constant and atomic positions to relax. Here, KFe₂As₂ is an example of extreme hole doping and if the experimental lattice constants are used, the biquadratic term is 6.3 meV,

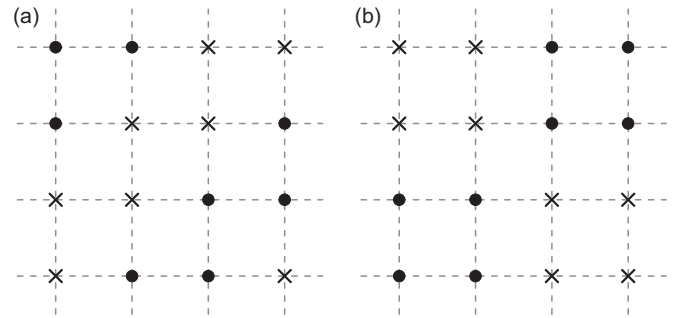


FIG. 3. The two magnetic configurations, in a 4×4 two-dimensional cell, which are degenerate for any pairwise Hamiltonian of arbitrary range. The closed circles correspond to spin-up moments and the crosses correspond to spin-down moments. (a) The double stripe configuration, which is the ground state of FeTe. (b) The square configuration.

in contrast to the vanishing biquadratic term inferred from extrapolating the VCA results discussed above. The Fe-Fe and Fe-As(Se) bond lengths, influenced by the hole-doping level, play a role in determining K . This is in line with the results of Ref. [16], where K for KFe₂Se₂ depended strongly on the internal coordinate z_{Se} .

Regarding the question of whether it is valid to assume that magnetic interactions can be accurately mapped to a pairwise Hamiltonian by just including an arbitrary number of terms, one can address this issue by comparing the two magnetic patterns shown in Fig. 3. It was pointed out [27] that these configurations are degenerate on the mean-field level for any Heisenberg model of arbitrary range. Being collinear, the configurations remain degenerate after the inclusion of the biquadratic interaction term, which can be lifted by either magnetoelastic coupling or by integrating out fluctuations [27]. We calculated the energy difference between these two configurations for FeTe using the experimental high-temperature structure (tetragonal) and found that the experimentally observed double stripe pattern is lower in energy than the square pattern by 8 meV/Fe, which is a small, but by no means irrelevant or negligible, number. The degeneracy is only lifted on the level of the fourth-order (square) ring exchange, which in the localized Hubbard limit is of the order of t^4/U^3 , as compared to the nearest-neighbor superexchange terms which are of the order of t^2/U .

Another consequence of attempting to map to the classical Heisenberg J_1 - J_2 - J_3 model is that it does not predict the double stripe or square pattern to be the ground state of FeTe, instead predicting spiral phases for large J_3 . In Ref. [27], it was pointed out that for some parameter range, collinear structures may be stabilized over the spiral ones because of quantum fluctuations. In contrast, our calculations clearly indicate that the sizable biquadratic interactions, present in the parent Fe-based HTSC compounds, completely exclude spiral phases already on the mean-field level. Moreover, DFT calculations strongly favor double stripes over squares, despite the fact that fluctuations work in the opposite way [27]. Our calculations strongly suggest that the fact that the experimental structure in FeTe appears to be double stripe is not related to magnetoelastic

coupling, as suggested in Ref. [27], but is instead due to itinerant effects not captured by the Heisenberg Hamiltonian.

Returning to the experiment from Ref. [19], we can use our results to comment upon the experimental data for the hole-doped compound $\text{Ba}_{0.76}\text{Na}_{0.24}\text{Fe}_2\text{As}_2$, which appeared consistent with a reentrant C_4 phase transition and also would require a change in the magnetic order to conform with the C_4 symmetry. The authors of Ref. [19] argue that their measurements are consistent with a noncollinear magnetic configuration, implying that the biquadratic term can change sign upon doping. However, our results do not support the proposed noncollinear magnetic configuration in Na-doped BaFe_2As_2 . Why might this be? One possibility is that, as discussed in Sec. I, there might not be a reentrant C_4 transition in Na-doped BaFe_2As_2 and so it would be unnecessary to argue for a change in the magnetic state. The argument for the reentrant C_4 transition is based on nuclear diffractogram measurements in which an apparent recombination of the nuclear Bragg peaks at low temperatures is observed. However, the Bragg peaks are quite broad, and so a reduction, but not a complete removal, of the orthorhombic distortion would also be consistent with the data. Another possibility is that the reentrant C_4 transition is not accompanied by a noncollinear magnetic configuration. The authors of Ref. [19] put forth a model of the C_4 transition with two magnetic configurations fitting well to measured x-ray diffraction data: the noncollinear configuration presented in the main body of the paper and also a collinear stripe state. The noncollinear model is preferred as it already has C_4 symmetry. The authors comment that a linear combination of spin density waves that produce stripes along the x and y directions also restores C_4 symmetry. Without more information, there is no reason to prefer one magnetic configuration over the other.

Therefore, in light of our results, there remain two plausible interpretations of the reentrant C_4 transition of $\text{Ba}_{0.76}\text{Na}_{0.24}\text{Fe}_2\text{As}_2$ described in Ref. [19]. The first is that the orthorhombic distortion of Na-doped BaFe_2As_2 is reduced at lower temperatures, but ultimately retains C_2 symmetry. This is the interpretation we prefer, as it is the simpler way in which C_2 symmetry would be preserved. A higher-resolution measurement of the temperature dependence of the nuclear Bragg peaks is necessary to rule this interpretation out. The second is that the C_4 transition does occur, but that the magnetic order remains striped and modulates between x - and y -oriented stripe patterns. Additional follow-up studies are necessary to ultimately resolve this question.

IV. CONCLUSIONS

We confirmed that biquadratic coupling is universally present in Fe-based superconductors. It is of the same order of magnitude as the superexchange interactions. In the studied materials, the biquadratic term is modestly affected by the softening of the magnetic moment, is influenced by the Fe-Fe and Fe-As bond lengths, and is dependent upon the doping, which underlines the biquadratic term's itinerant origin. We find that even in the case of extreme hole doping, no experimentally realized material exhibits a change of sign in the biquadratic term, so the collinear AFM stripe state is energetically preferred in all instances. Therefore, the

apparent experimental observation of a reentrant C_4 transition in Na-doped BaFe_2As_2 is likely to be an artifact due to the inaccessibility of measuring the C_2 symmetry at low temperatures with the experimental tools.

Our results show that in the realm of Fe-based superconductors, the naive Heisenberg model is a rather poor approximation. The biquadratic exchange plays an essential role and cannot be neglected in any model calculation describing these compounds. In addition, there are deviations, as observed for FeTe, from the general pairwise interaction model for linear and biquadratic terms of an arbitrary range. In FeTe, it is these terms that stabilize the experimentally observed double stripe in the calculations, and not the magnetoelastic coupling, as conjectured before [27]. It remains to be seen whether these interesting features are specific to the parent compounds of Fe-based HTSCs or are more common than previously expected. Further calculations and studies should aid in answering this question.

ACKNOWLEDGMENTS

I.I.M. acknowledges funding from the Office of Naval Research (ONR) through the Naval Research Laboratory's Basic Research Program. J.V. acknowledges the support of the Office of Naval Research Summer Faculty Research Program. J.G. acknowledges the support of the NRC program at NRL.

APPENDIX A: VALIDITY OF THE VIRTUAL CRYSTAL APPROXIMATION (VCA)

We confirmed the validity of the VCA by doing the following test calculations using BaFe_2As_2 . To begin, we directly substituted a Na atom for a Ba atom (the two Ba sites are equivalent via symmetry), keeping the lattice and internal parameters set to the values taken from experiment, and calculated $\Delta E(\pi/2)$. For $\text{Ba}_{0.5}\text{Na}_{0.5}\text{Fe}_2\text{As}_2$, we obtained $\Delta E(\pi/2) = 11.4$ meV, which is about a factor of two smaller than the VCA $x = 0.5$ result of 21.5 meV.

To see how structural deformations affect $\Delta E(\theta)$, we relaxed the structures in the pseudopotential-based software suite VASP [28,29]. In VASP, we used projector augmented wave (PAW) pseudopotentials [30,31] and the Perdew-Burke-Ernzerhof generalized gradient approximation [24] to DFT. Our BaFe_2As_2 calculations in the main text took the internal parameter z_{As} from experiment. We wanted to make a proper comparison between VCA and a relaxed structure with Na substitutions, so in order to do this we relaxed the internal parameter z_{As} for both undoped BaFe_2As_2 and doped $\text{Ba}_{0.5}\text{Na}_{0.5}\text{Fe}_2\text{As}_2$ in VASP and imported the coordinates into ELK. We then calculated $\Delta E(\pi/2)$ for BaFe_2As_2 in the VCA with $x = 0.5$ using the relaxed atomic positions found for undoped BaFe_2As_2 , and then calculated $\Delta E(\pi/2)$ for $\text{Ba}_{0.5}\text{Na}_{0.5}\text{Fe}_2\text{As}_2$ using both the relaxed structure for undoped BaFe_2As_2 and the relaxed structure for $\text{Ba}_{0.5}\text{Na}_{0.5}\text{Fe}_2\text{As}_2$. The VCA result with the undoped structure is $\Delta E(\pi/2) = 10.3$ meV. The $\text{Ba}_{0.5}\text{Na}_{0.5}\text{Fe}_2\text{As}_2$ result using the relaxed undoped structure is $\Delta E(\pi/2) = 3.28$ meV and the result using the relaxed structure for $\text{Ba}_{0.5}\text{Na}_{0.5}\text{Fe}_2\text{As}_2$ is $\Delta E(\pi/2) = 7.58$ meV. If the cell volume of $\text{Ba}_{0.5}\text{Na}_{0.5}\text{Fe}_2\text{As}_2$ is fixed

and both the internal parameter z_{As} and a and c parameters are relaxed and then imported into ELK, then $\Delta E(\pi/2) = 3.08$ meV for $\text{Ba}_{0.5}\text{Na}_{0.5}\text{Fe}_2\text{As}_2$.

Overall, the VCA overestimates $\Delta E(\theta)$, but this does not affect the qualitative behavior, i.e., the biquadratic term K does not change sign. Furthermore, using relaxed structures

illustrates the sensitivity of the biquadratic interaction to the distance between the Fe and As(Se) planes, but these subtle changes do not materially change the overall trends. We conclude that the VCA is an appropriate method for investigating whether doping can affect the qualitative behavior of the biquadratic term.

-
- [1] A. Chubukov, *Ann. Rev. Condens. Matter Phys.* **3**, 57 (2012).
- [2] P. J. Hirschfeld, M. M. Korshunov, and I. I. Mazin, *Rep. Prog. Phys.* **75**, 124508 (2011).
- [3] M. D. Johannes and I. I. Mazin, *Phys. Rev. B* **79**, 220510(R) (2009).
- [4] I. I. Mazin and M. D. Johannes, *Nat. Phys.* **5**, 141 (2009).
- [5] P. Chandra, P. Coleman, and A. I. Larkin, *Phys. Rev. Lett.* **64**, 88 (1990).
- [6] C. Xu, M. Müller, and S. Sachdev, *Phys. Rev. B* **78**, 020501(R) (2008).
- [7] C. Fang, H. Yao, W.-F. Tsai, J. P. Hu, and S. A. Kivelson, *Phys. Rev. B* **77**, 224509 (2008).
- [8] I. I. Mazin and J. Schmalian, *Physica C* **469**, 614 (2009).
- [9] S. Kasahara, H. J. Shi, K. Hashimoto, S. Tonegawa, Y. Mizukami, T. Shibauchi, K. Sugimoto, T. Fukuda, T. Terashima, A. H. Nevidomskyy, and Y. Matsuda, *Nature (London)* **486**, 382 (2012).
- [10] M. D. Watson, A. McCollam, S. F. Blake, D. Vignolles, L. Drigo, I. I. Mazin, D. Guterding, H. O. Jeschke, R. Valenti, N. Ni, R. Cava, and A. I. Coldea, [arXiv:1310.3728](https://arxiv.org/abs/1310.3728).
- [11] S. Li, C. de la Cruz, Q. Huang, Y. Chen, J. W. Lynn, J. Hu, Y.-L. Huang, F.-C. Hsu, K.-W. Yeh, M.-K. Wu, and P. Dai, *Phys. Rev. B* **79**, 054503 (2009).
- [12] Z. P. Yin, S. Lebegue, M. J. Han, B. P. Neal, S. Y. Savrasov, and W. E. Pickett, *Phys. Rev. Lett.* **101**, 047001 (2008).
- [13] K. D. Belashchenko and V. P. Antropov, *Phys. Rev. B* **78**, 212505 (2008).
- [14] A. N. Yaresko, G.-Q. Liu, V. N. Antonov, and O. K. Andersen, *Phys. Rev. B* **79**, 144421 (2009).
- [15] A. L. Wysocki, K. D. Belashchenko, and V. P. Antropov, *Nat. Phys.* **7**, 485 (2011).
- [16] A. L. Wysocki, K. D. Belashchenko, L. Ke, M. van Schlipfhaarde, and V. P. Antropov, *J. Phys.: Conf. Series* **449**, 012024 (2013).
- [17] C.-C. Lee, W.-G. Yin, and W. Ku, *Phys. Rev. Lett.* **103**, 267001 (2009).
- [18] W.-G. Yin, C.-C. Lee, and W. Ku, *Phys. Rev. Lett.* **105**, 107004 (2010).
- [19] S. Avci, O. Chmaissem, S. Rosenkranz, J. M. Allred, I. Eremin, A. V. Chubukov, D.-Y. Chung, M. G. Kanatzidis, J.-P. Castellán, J. A. Schlueter, H. Claus, D. D. Khalyavin, P. Manuel, A. Daoud-Aladine, and R. Osborn, [arXiv:1303.2647](https://arxiv.org/abs/1303.2647).
- [20] R. M. Fernandes, A. V. Chubukov, J. Knolle, I. Eremin, and J. Schmalian, *Phys. Rev. B* **85**, 024534 (2012).
- [21] The crystal structure parameters for FeSe (lattice parameters and internal parameter z_{Se}) are taken from the doped compound $\text{FeSe}_{0.5}\text{Te}_{0.5}$. Doping with Te has the primary effect of changing the crystal structure, which drives the superconducting transition.
- [22] C. de la Cruz, Q. Huang, J. W. Lynn, J. Li, W. Ratcliff, II, J. L. Zarestky, H. A. Mook, G. F. Chen, J. L. Luo, N. L. Wang, and P. Dai, *Nature (London)* **453**, 899 (2008).
- [23] ELK FP-LAPW code, <http://elk.sourceforge.net/>.
- [24] J. P. Perdew, K. Burke, and M. Ernzerhof, *Phys. Rev. Lett.* **77**, 3865 (1996).
- [25] In their calculations, the authors of Ref. [16] broke the $I4/mmm$ symmetry and constrained the moments along the c -axis direction to be collinear in order to suppress the interplanar interaction term in Eq. (3). Therefore, their $\Delta E(\theta)$ curves are symmetric about $\theta = \pi/2$, while ours are not.
- [26] X. Ding, D. Fang, Z. Wang, H. Yang, J. Liu, Q. Deng, G. Ma, C. Meng, Y. Hu, and H.-H. Wen, *Nat. Commun.* **4**, 1897 (2013).
- [27] S. Ducatman, N. B. Perkins, and A. Chubukov, *Phys. Rev. Lett.* **109**, 157206 (2012).
- [28] G. Kresse and J. Hafner, *Phys. Rev. B* **47**, 558 (1993).
- [29] G. Kresse and J. Furthmüller, *Phys. Rev. B* **54**, 11169 (1996).
- [30] P. E. Blöchl, *Phys. Rev. B* **50**, 17953 (1994).
- [31] G. Kresse and D. Joubert, *Phys. Rev. B* **59**, 1758 (1999).